Scattering by quasi-symmetric pipes

Michael Carley[a)]
Department of Mechanical Engineering, University of Bath, Bath BA2 7AY, England

(Received 3 June 2005; revised 7 October 2005; accepted 29 November 2005)

A hypersingular boundary integral method for the prediction of radiation from a straight circular pipe with arbitrary end profile has been developed. The technique represents an extension of established procedures for axisymmetric pipes with the addition of recent advances in special function and quadrature theory to simplify the implementation. The resulting code is applied to two sample problems: first, the prediction of radiation of a plane wave mode from a pipe with its ends cut by an inclined plane, representing the "scarfed intake" proposed for reduction of aircraft engine noise. Second, the method is used to examine scattering of an incident azimuthal mode by a multi-lobed profile, characteristic of the "chevron" nozzles proposed for jet engine exhausts.
 [DOI: 10.1121/1.2159432]

PACS number(s): 43.20.−f, 43.20.Mv, 43.20.Rz [MO] Pages: 817–823

I. INTRODUCTION

This paper addresses the problem of calculating the sound radiated from a straight, circular section pipe with an arbitrary end profile, motivated by two features proposed for modern aero-engines. The first, "scarfing," has been proposed as a means of redirecting the fan noise radiated from the intake of an engine so that the noise on the ground is reduced.[1] The second is the "chevron nozzle" in which an asymmetric exhaust nozzle is used to modify the flow so that the noise source is reduced.[2] In such an approach, the main reason for the noise reduction appears to be the modification of the flow and consequent effect on the aerodynamic source terms, but an examination of the purely acoustic effect of the chevron nozzle is still of some interest, if only for its connection with the instabilities of the jet shear layer.[3]

The method to be developed is a relatively conventional technique for scattering from straight circular pipes as used by a number of researchers in the past,[4–6] who employed a hypersingular integral equation to solve the scattering problem. The essential difference is that in this paper, the approach is extended to a pipe with end profiles given by an arbitrary function of azimuthal angle on the pipe. In addition, recent advances in quadrature theory[7] and special functions[8] are used to handle the hypersingular terms which arise in the integral equation. The central part of the method is the decomposition of the integral equation into a set of coupled equations for the amplitudes of the azimuthal modes of the surface pressure jump. This makes the problem into one similar to that in engine noise where a duct mode interacts with the internal stationary vanes in an engine[9] with the role of the stators being played by the duct end profile.

The problem of scattering by scarfed duct terminations has been studied with asymptotic methods being applied to the case of low-frequency radiation from ducts with small scarf angle[1] and ray theory to high-frequency radiation from ducts of arbitrary scarf angle.[10] There is then a gap in the literature which this paper aims to fill: the problem of relatively low-frequency scattering from duct terminations with large scarf angle. Since the general termination problem is no more difficult numerically than the simple scarfed duct problem, results for the chevron termination case will also be presented.

II. NUMERICAL TECHNIQUE

An integral equation method based on existing techniques is now developed for the solution of the problem of scattering by straight, circular pipes with arbitrary end profiles. The formulation yields a set of coupled equations for azimuthal mode amplitudes on a distorted circular source, not unlike the "wobbling modes" studied in propeller noise.[11,12] The resulting equations include a hypersingular integral which is evaluated using recently developed quadratures, easing the analysis of the integral kernel.

A. Formulation

The geometry of the system is shown in Fig. 1. A zero-thickness, circular section, straight pipe extending from $z=a$ to $z=b$ is subjected to an incident acoustic field p_{inc}. The pipe ends have identical azimuth-dependent profiles $\epsilon w(\theta)$ where ϵ is the profile depth and $w(\theta)$ is the shape; $-\sin\theta$ for a linear scarf. A cylindrical coordinate system (r,θ,z) is used for calculations with position on the pipe surface given by

$$x = r_1 \cos\theta_1, \quad y = r_1 \sin\theta_1, \quad z = z_1 + \epsilon w(\theta_1),$$

where the subscript 1 indicates variables of integration. The profile shape $\epsilon w(\theta_1)$ is imposed at all axial positions so that the formulation of the integral equations will involve analysis of radiation from distorted ring sources. For the directivity plots shown later, spherical coordinates (R,θ,ϕ) are used and are indicated in Fig. 1.

The total acoustic field is made up of the incident field and that radiated by the pipe surface. Using a standard approach,[4–6] the solution for the scattered field is computed via the pressure jump Δp across the surface, which acts as a distribution of radial dipoles:

[a)]Electronic mail: m.j.carley@bath.ac.uk

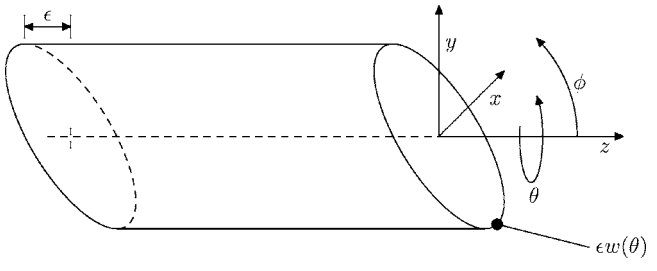

FIG. 1. Coordinate systems for scarfed cylinder.

$$p(r,\theta,z) = p_{\text{inc}} + \int\int \Delta p(\theta_1,z_1)\frac{\partial}{\partial r_1}\frac{e^{jkR}}{4\pi R}\,dS, \tag{1}$$

where S is the scattering surface, R is the source-observer distance, k is the acoustic wave number, and time dependence $\exp -j\omega t$ has been assumed.

To find Δp, the integral equation is solved subject to the boundary condition that the pressure gradient on the surface be identically zero:

$$-\frac{\partial p_{\text{inc}}}{\partial r} = \int\int \Delta p(\theta_1,z_1)\frac{\partial^2}{\partial r\,\partial r_1}\frac{e^{jkR}}{4\pi R}\,dS. \tag{2}$$

Because the two ends of the pipe have identical profiles, the transformation of the integral has unit Jacobian and Eq. (2) can be written

$$-\frac{\partial p_{\text{inc}}}{\partial r} = \int_a^b\int_0^{2\pi} \Delta p(\theta_1,z_1)\frac{\partial^2}{\partial r\,\partial r_1}\frac{e^{jkR}}{4\pi R}\,d\theta_1\,dz_1. \tag{3}$$

The standard approach[4–6] to solving the integral equation for Δp is to decompose it into a suitable set of basis functions and compute the coefficients of these functions subject to the boundary conditions. In this case, Δp is decomposed into azimuthal modes in $\exp jn\theta$ and Chebyshev polynomials of the second kind U_n so that

$$\Delta p(\theta_1,z_1) = \sum_{m=-\infty}^{\infty}\sum_{n=0}^{N} Q_{nm}e^{jm\theta_1}U_n\left(\frac{z_1-\bar{z}}{L/2}\right) \times (z_1-a)^{1/2}(b-z_1)^{1/2}, \tag{4}$$

where the pipe length $L=b-a$. Inserting Eq. (4) into Eq. (3), gives an integral equation for the coefficients Q_{nm}:

$$-\frac{\partial p_{\text{inc}}}{\partial r} = \sum_m Q_{nm}\sum_{n=0}^{N}\left(\frac{L}{2}\right)^2\int_{-1}^{1} U_n(t)(1-t^2)^{1/2}\frac{\partial^2 g_m}{\partial r\,\partial r_1}\,dt, \tag{5}$$

where

$$g_m = \int_0^{2\pi}\frac{e^{j(kR+m\theta_1)}}{4\pi R}\,d\theta_1,$$

$$\bar{z} = \frac{a+b}{2}, \quad z_1 = \bar{z} + \frac{L}{2}t.$$

Equation (5) is a set of coupled equations which must be solved for all azimuthal mode orders simultaneously, with the required mode orders m to be prescribed in advance.

B. Green's function analysis

To numerically evaluate the integral of Eq. (5), the singular part of the kernel must be isolated and analyzed. This is most easily handled using some recent results in the theory of elliptic-type integrals. Following Dawson,[13] the Green's function g_m is broken into a bounded and a singular part:

$$g_m = g_m^{(b)} + g_m^{(s)}, \tag{6a}$$

$$g_m^{(b)} = \int_0^{2\pi} e^{jm\theta_1}\frac{e^{jkR_\epsilon} - 1 - jkR_\epsilon + k^2R_\epsilon^2/2}{4\pi R_\epsilon}\,d\theta_1, \tag{6b}$$

$$g_m^{(s)} = \int_0^{2\pi} e^{jm\theta_1}\frac{1 + jkR_\epsilon - k^2R_\epsilon^2/2}{4\pi R_\epsilon}\,d\theta_1, \tag{6c}$$

$$R_\epsilon^2 = r^2 + r_1^2 - 2rr_1\cos(\theta-\theta_1) + (z - z_1 + \epsilon\Delta w)^2,$$

$$\Delta w = w(\theta) - w(\theta_1).$$

The kernel of Eq. (5) is found by differentiation so that the bounded part can be written

$$\begin{aligned}\frac{\partial^2 g_m^{(b)}}{\partial r\,\partial r_1} = \int_0^{2\pi}\frac{e^{jm\theta_1}}{4\pi}\Bigg[&\frac{2}{R_\epsilon^3}(e^{jkR_\epsilon} - 1 - jkR_\epsilon + k^2R_\epsilon^2/2) \\ &- \frac{jk}{R_\epsilon^2}(e^{jkR_\epsilon} - 1 - jkR_\epsilon) - \frac{k^2}{R_\epsilon}(e^{jkR_\epsilon} - 1)\Bigg]\frac{\partial R_\epsilon}{\partial r}\frac{\partial R_\epsilon}{\partial r_1} \\ &+ \frac{e^{jm\theta_1}}{4\pi}\Bigg[\frac{jk}{R_\epsilon}(e^{jkR_\epsilon} - 1 - jkR_\epsilon) \\ &- \frac{1}{R_\epsilon^2}(e^{jkR_\epsilon} - 1 - jkR_\epsilon + k^2R_\epsilon^2/2)\Bigg]\frac{\partial^2 R_\epsilon^2}{\partial r\,\partial r_1}\,d\theta_1,\end{aligned} \tag{7}$$

and it is clear that all terms in the integrand have a finite limit as the field point approaches the source position.

The singular kernel must be treated differently to extract the leading order singularity. The aim is to make use of existing results for axisymmetric systems, as robust techniques are available for solving such problems. Expanding $g_m^{(s)}$ as a power series

$$\frac{\partial^2 g_m^{(s)}}{\partial r\,\partial r_1} = \sum_{u=0}^{\infty}\frac{\epsilon^u}{u!}\frac{\partial^u}{\partial\epsilon^u}\left(\frac{\partial^2 g_m^{(s)}}{\partial r\,\partial r_1}\right)\Bigg|_{\epsilon=0} \tag{8}$$

which can be rewritten

$$\frac{\partial^2 g_m^{(s)}}{\partial r\,\partial r_1} = \sum_{u=0}^{\infty}\frac{(\epsilon\Delta w)^u}{u!}\frac{\partial^u}{\partial z^u}\left(\frac{\partial^2 g_m^{(s)}}{\partial r\,\partial r_1}\right)\Bigg|_{\epsilon=0}, \tag{9}$$

because z and ϵ only occur in the combination $(z-z_1+\epsilon\Delta w)$.

Because $\epsilon=0$ corresponds to the axisymmetric problem, the singular kernel can be computed using established results. The terms which must be handled are of the form $\exp jm\theta_1/R_\epsilon^n$ which can be written

$$\frac{1}{R_\epsilon^2} = \sum_{u=0}^{\infty} \frac{(\epsilon \Delta w)^u}{u!} \frac{\partial^\mu}{\partial z^u} \frac{1}{R_0^n}, \tag{10}$$

where R_0 is R_ϵ evaluated at $\epsilon=0$. The terms related to the end profile $w(\theta)$ are expanded in a Fourier series:

$$(\Delta w)^u = \sum_{p,q} W_{pq}^{(u)} e^{jp\theta} e^{jp\theta_1},$$

where nonzero values of $W_{pq}^{(u)}$ are included in the summation and

$$\frac{1}{R_\epsilon^n} = \sum_{u=0}^{\infty} \frac{\epsilon^u}{u!} \frac{\partial^\mu}{\partial z^u} \sum_{p,q} W_{pq}^{(u)} e^{jp\theta} \frac{e^{jq\theta_1}}{R_0^n}. \tag{11}$$

Integration of Eq. (11) yields

$$\int_0^{2\pi} \frac{e^{jm\theta_1}}{R_\epsilon^n} d\theta_1 = \sum_{u=0}^{\infty} \frac{\epsilon^u}{u!} \frac{\partial^\mu}{\partial z^u} \sum_{p,q} W_{pq}^{(u)} e^{jp\theta} \int_0^{2\pi} \frac{e^{j(m+q)\theta_1}}{R_0^n} d\theta_1.$$

This can be simplified as follows. Using the substitution $\theta_1' = \theta - \theta_1$

$$\int_0^{2\pi} \frac{e^{jm\theta_1}}{[r^2 + r_1^2 - 2rr_1 \cos(\theta - \theta_1) + (z - z_1)^2]^{n/2}} d\theta_1$$

$$= e^{jm\theta} \int_0^{2\pi} \frac{\cos m\theta_1'}{[r^2 + r_1^2 - 2rr_1 \cos\theta_1' + (z - z_1)^2]^{n/2}} d\theta_1'$$

$$= e^{jm\theta} \int_0^{2\pi} \frac{\cos 2m\phi}{[(r + r_1)^2 + (z - z_1)^2 - 4rr_1 \cos^2\phi]^{n/2}} d\phi$$

after the substitution $\theta' = 2\phi$. Then, setting

$$\rho^2 = (r + r_1)^2 + (z - z_1)^2, \quad \lambda^2 = \frac{4rr_1}{\rho^2},$$

and defining

$$H(n,m,\lambda) = \int_0^{2\pi} \frac{\cos 2m\phi}{(1 - \lambda^2 \cos^2\phi)^{n/2}} d\phi, \tag{12}$$

Eq. (11) becomes

$$\int_0^{2\pi} \frac{e^{jm\theta_1}}{R_\epsilon^n} d\theta_1 = \sum_{u=0}^{\infty} \frac{\epsilon^u}{u!} \frac{\partial^\mu}{\partial z^u} \sum_{p,q} W_{pq}^{(u)} e^{j(p+q+m)\theta} \frac{H(n,m+q,\lambda)}{\rho^n}. \tag{13}$$

The elliptic-type integral $H(n,m,\lambda)$ has been extensively analyzed due to its importance in radiation problems. In particular, recursion relations have been derived for its efficient evaluation and an asymptotic series exists for the case where $n=2n'+1$, covering the cases of interest in this paper:[8]

$$H(2n'+1,m,\lambda) = \frac{\lambda^{2m} \lambda'^{-2n'}}{(1/2)_{n'}} \times \left(\sum_{k=0}^{n'-1} (-1)^k C_k (n' - 1 - k)!\, \lambda'^{2k} + (-1)^{n'} \sum_{k=n'}^{\infty} \frac{C_k}{(k - n')!} h_k(\lambda') \lambda'^{2k} \right), \tag{14}$$

where

$$C_k = \left(\frac{1}{2} + m\right)_k \left(\frac{1}{2} + m - n'\right)_k / k!,$$

$$h_k(\lambda') = \psi(1 + k) + \psi(1 + k - n') - \psi\left(\frac{1}{2} + m + k\right) - \psi\left(\frac{1}{2} + m - n' + k\right) - 2 \log \lambda',$$

$$\lambda' = (1 - \lambda^2)^{1/2},$$

ψ is the logarithmic derivative of the gamma function, and $(a)_n$ is Pochammer's symbol. The asymptotic series, as well as being useful in evaluating the kernel proper, is also useful in that it gives the strength of the leading order singularity as $\lambda \to 1$.

Differentiating Eq. (6c) with $\epsilon=0$,

$$K_m^{(s)} = \left. \frac{\partial^2 g_m^{(s)}}{\partial r\, \partial r_1} \right|_{\epsilon=0} = \frac{1}{8\pi} \frac{r^2 + r_1^2}{rr_1} \frac{H(3,m,\lambda)}{\rho^3} + \frac{3}{16\pi} \frac{1}{rr_1} [(z - z_1)^4 - (r - r_1)^2 (r + r_1)^2] \times \frac{H(5,m,\lambda)}{\rho^5} + \frac{1}{8\pi} \frac{1}{rr_1} [r^2 + r_1^2 - 2(z - z_1)^2] \times \frac{H(3,m,\lambda)}{\rho^3} + \frac{1}{16\pi} \frac{1}{rr_1} \frac{H(1,m,\lambda)}{\rho^1} + \frac{k^2}{32\pi} \frac{1}{rr_1} [(z - z_1)^4 - (r - r_1)^2 (r + r_1)^2] \frac{H(3,m,\lambda)}{\rho^3} + \frac{k^2}{16\pi} \frac{1}{rr_1} (r + r_1)^2 \frac{H(1,m,\lambda)}{\rho^1} - \frac{k^2}{32\pi} \frac{1}{rr_1} \frac{H(-1,m,\lambda)}{\rho^{-1}} - \frac{k^2}{8\pi} \frac{1}{rr_1} \frac{H(1,m,\lambda)}{\rho^1}, \tag{15}$$

so that the asymmetric kernel becomes

$$\frac{\partial^2 g_m^{(s)}}{\partial r\, \partial r_1} = \sum_{u=0}^{\infty} \frac{\epsilon^u}{u!} \frac{\partial^\mu}{\partial z^u} \sum_{p,q} W_{pq}^{(u)} e^{j(p+q+m)\theta} K_{m+q}^{(s)}. \tag{16}$$

We note in passing that the substitution $r=r_1 \equiv 1$ has not been made in Eq. (15) in order to allow the numerical procedures to be checked by evaluating the kernel with $r \neq r_1$.

Finally, inserting Eq. (16) into the integral equation and moving the differentiations from under the integral sign

$$\int_{-1}^{1} \frac{\partial^2 g_m^{(s)}}{\partial r\, \partial r_1} U_n(t)(1-t^2)^{1/2}\, \mathrm{d}t$$

$$= \sum_{u=0}^{\infty} \frac{\epsilon^u}{u!} \frac{\partial^u}{\partial z^u} \sum_{p,q} W_{pq}^{(u)} \mathrm{e}^{\mathrm{j}(p+q+m)\theta} \times \int_{-1}^{1} K_{m+q}^{(s)} U_n(t)(1-t^2)^{1/2}\, \mathrm{d}t. \tag{17}$$

C. Hypersingular kernel

The singular part of the kernel requires special treatment as standard numerical integration techniques will not work. The first step is to isolate the most singular term. This can be done most easily using the asymptotic series, Eq. (14). With $r=r_1 \equiv 1$, the most strongly singular term is the first term in

$$\frac{1}{4\pi} \frac{H(3,m,\lambda)}{\rho^3}.$$

Setting

$$\lambda'^2 = \frac{4}{4+(z-z_1)^2},$$

the leading order singularity is

$$\frac{1}{4\pi} \frac{H(3,m,\lambda)}{\rho^3} \sim \frac{1}{2\pi} \frac{1}{(z-z_1)^2}, \quad z \to z_1,$$

which can also be derived using small argument methods.[6]

This result means that the integrand has hypersingular behavior as $z \to z_1$ and the integral of Eq. (5) must be interpreted in the Hadamard finite-part sense.[14–16] A number of approaches exist for the evaluation of finite-part integrals but the most convenient for our purposes is the Gaussian-type quadrature of Korsunsky,[7] which is a special case of the rules derived by Monegato.[17] This quadrature is particularly good for integral equations based on Chebyshev polynomial expansions where the kernel is difficult to analyze in detail. When the kernel can be written in the form

$$K(t,x) = \frac{1}{(t-x)^2} + k(t,x),$$

the quadrature rule of order n is

$$\fint_{-1}^{1} K(t,x) g(t)(1-t^2)^{1/2} \mathrm{d}t \approx \pi \sum_{i=1}^{n} \left(\frac{1-t_i^2}{n+1} K(t_i,x_k) + \frac{1-t_i^2}{t_i-x_k} \frac{(-1)^{i+k}}{(1-x_k^2)^{1/2}} \right) g(t_i), \tag{18}$$

$$t_i = \cos\frac{i\pi}{n+1} \quad \text{and} \quad x_k = \cos\frac{(2k-1)\pi}{2(n+1)}, \quad k = 1, \ldots, n+1,$$

where $\fint$ denotes the finite-part integral. Note that $k(t,x)$ may contain singularities up to order 1 and these will be evaluated as Cauchy principal values.

D. Differentiation of kernel

Equation (17) requires that the integral in it be differentiated with respect to the axial coordinate. The collocation points are defined by Eq. (18) and lie in the range $-1 < x < 1$ where x is the transformed variable inside the range of integration. Differentiation with respect to the physical variable z is then simply a scaled version of differentiation with respect to x:

$$\frac{\partial}{\partial z} = \frac{2}{L} \frac{\partial}{\partial x}.$$

In assembling the equations, I is evaluated at the collocation points so that we start from a set of data (x_k, I_k). In order to perform the differentiation, we fit a set of Chebyshev polynomials of the first kind to the data and use the coefficients of the series to evaluate the derivative. The Chebyshev expansion of a function is given by

$$I(x) = \sum_{m=0}^{m=M} a_m T_m(x), \tag{19}$$

where, by the orthogonality relation for Chebyshev polynomials,[18]

$$a_0 = \frac{1}{\pi} \int_{-1}^{1} I(x)(1-x^2)^{-1/2}\, \mathrm{d}x,$$

$$a_m = \frac{2}{\pi} \int_{-1}^{1} I(x) T_m(x)(1-x^2)^{-1/2}\, \mathrm{d}x, \quad m \neq 0.$$

Because of the location of the collocation points x_k, it is convenient to transform the integrals for the Chebyshev coefficients. Setting $x = \cos\phi$ and noting that $T_m(x) \equiv \cos m\phi$,

$$a_m = \frac{2}{\pi} \int_0^{\pi} I(\cos\phi) \cos m\phi\, \mathrm{d}\phi.$$

The integral has been evaluated at the collocation points given by Eq. (18) so that the data are equally spaced in ϕ and

$$a_0 \approx \frac{1}{2n} \sum_{k=0}^{n} I_k, \tag{20a}$$

$$a_m \approx \frac{1}{n} \sum_{k=0}^{n} I_k T_m(x_k), \quad m \neq 0. \tag{20b}$$

To evaluate the derivative, we use the formula $\mathrm{d}T_m/\mathrm{d}x = mU_{m-1}(x)$ and

$$\frac{\partial I}{\partial x} = \sum_{m=0}^{M} m a_m U_{m-1}(x), \tag{21}$$

which can be differentiated in turn to evaluate the higher derivatives.

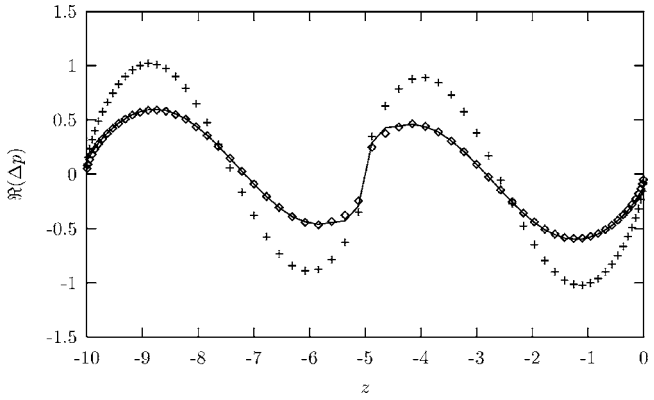

FIG. 2. Convergence of solution for scarf angle 30° (ϵ=0.58): surface pressure jump $\mathcal{R}(\Delta p)$ against the axial coordinate at $\theta=\pi/2$; cross: first order; diamond: third order; solid line: fifth order.

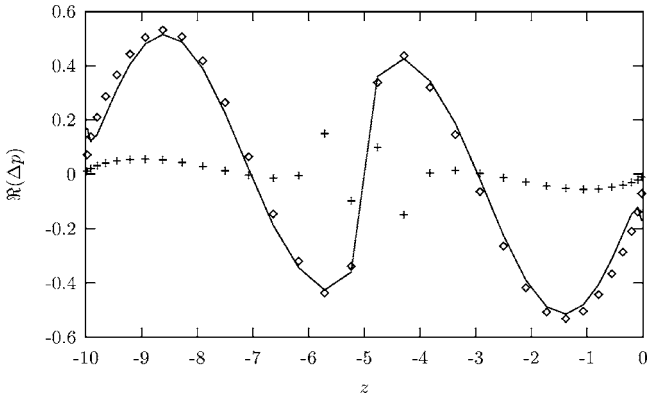

FIG. 3. Convergence of solution for scarf angle 45° (ϵ=1.0): surface pressure jump $\mathcal{R}(\Delta p)$ against the axial coordinate at $\theta=\pi/2$; cross: first order; diamond: third order; solid line: fifth order.

E. Implementation

The implementation of the method follows the sequence given above. The incident field azimuthal order is specified as are the azimuthal orders of the modes to be included in the scattering calculation. For a field of order m incident on a linear scarf, the required modes will be $m\pm u$, where $u=0,1,\ldots,U$ where, in the results shown here, U is the maximum order of the expansion in ϵ. The profile $w(\theta)$ is specified, allowing $W_{pq}^{(u)}$ to be computed using a two-dimensional Fourier transform.[19]

For M azimuthal modes, the boundary conditions are imposed at angular positions $\theta_i=i2\pi/M$, where $i=0,\ldots,M-1$, and at axial positions found from the quadrature rule, Eq. (18):

$$z_k=\bar{z}+\frac{L}{2}x_k+\epsilon w(\theta_i).$$

This yields a well-posed system of equations for Q_{nm} which can be used in Eq. (1) to calculate the scattered pressure.

III. RESULTS

Before presenting some sample results of the method, the numerical performance of the technique is analyzed. The important property of the method is its convergence behavior with respect to ϵ and the order of the solution, i.e., the highest power of ϵ considered. Figure 2 presents results for a linear scarf with ϵ=0.58 and k=1.0, computed using terms up to $O(\epsilon)$, $O(\epsilon^3)$, and $O(\epsilon^5)$, a case considered in Sec. III A. The number of azimuthal modes included in the solution is increased as the order of the calculation rises. Figure 2 shows the real part of the computed surface pressure jump $\mathcal{R}(\Delta p)$ against the surface axial coordinate. The solid curve shows the $O(\epsilon^5)$ solution while the diamonds and crosses show the $O(\epsilon^3)$ and $O(\epsilon)$ solutions, respectively. It can be seen that the third- and fifth-order solutions coincide. Figure 3 shows equivalent data for ϵ=1, the most extreme case computed in this paper, and the behavior with ϵ is seen to be similar: poor results if only terms up to $O(\epsilon)$ are included but convergence thereafter. The behavior of the solution for smaller ϵ was similar and so all of the results which follow have been computed to order ϵ^5.

The second issue is that of the time required to solve a problem. Figure 4 shows the computational time required to assemble the matrix for solution of the linear scarf problem at ϵ=1 with different numbers of modes included. The data were generated by increasing the order of ϵ and the number of modes simultaneously. The computational time shown has been scaled on the time required in the single mode case, i.e., the axisymmetric problem. There is no clear-cut variation in computational time with the number of modes N, but it does appear to be roughly N^2, as shown by the superimposed quadratic fit.

A. Plane wave-linear scarf interaction

The first problem considered is that of radiation from a pipe with a linear scarf. In recent papers, asymptotic analysis has been applied to low-frequency scattering by ducts with a small scarf angle[1] and ray theory to high-frequency radiation from ducts of arbitrary scarf angle.[10] It has been noted,[1] however, that a numerical solution is required when both the scarf angle and the wave number are $O(1)$. For this reason, the nondimensional wave number k=1 and the radiated field is calculated for scarf angles of 0°, 15°, 30°, and 45° ($\epsilon=0,0.27,0.58,1.0$). The incident field is generated by a ring of axial dipoles of unit strength at radius $\frac{1}{2}$ placed at $z=-5$ in a duct of length 10 with $a=-10$ and $b=0$. The next cut-on

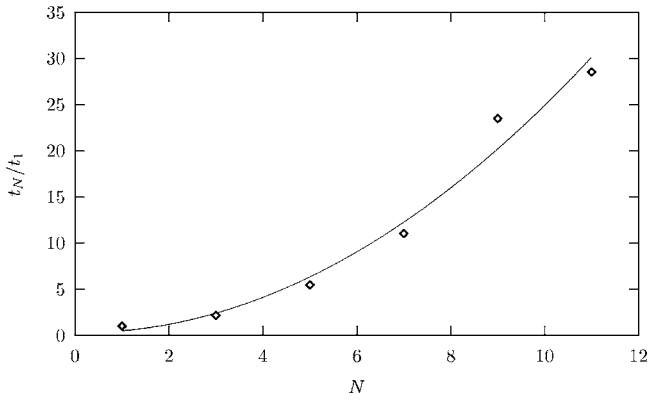

FIG. 4. Computational time for matrix assembly against number of modes included. Time has been scaled on time for single mode (axisymmetric problem). Diamonds: computation time; solid line: quadratic polynomial fit.

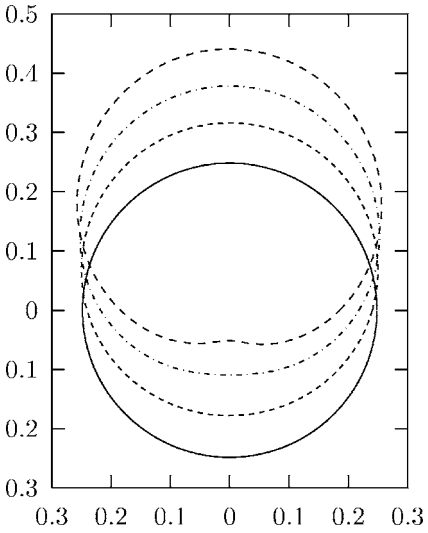

FIG. 5. Polar plot of $|p|^2R^2$ against θ at $\phi=\pi/4$ for an axisymmetric field incident on a linear scarf. Wave number $k=1.0$; scarf angles 0°, 15°, 30°, and 45°, shown as solid, dashed, dot-dashed, and dashed lines, respectively.

wave number is $k=3.832$ so that only the plane mode propagates.[20] Far-field directivities are plotted as $|p|^2R^2$ where the radial coordinate R is centered on the nominal center of the duct face at $z=0$. In performing the calculation $R=20$.

Figure 5 shows the normalized sound power at constant $\phi=\pi/4$ with azimuthal angle θ varying. The solid line represents the axisymmetric case $\epsilon=0$ and the directivity pattern moves up as the scarf angle increases. As in Fig. 3 of Peake's work,[1] the scarfing has shifted the directivity so that the noise below the duct is reduced and that above it increased—precisely the aim of scarfing.

Figure 6 shows the directivity in a vertical plane through the duct centerline. The field ahead of the inlet plane is composed of a narrow lobe near the vertical and a broader one along the axis. Behind the inlet plane, there is a second set of lobes. These are the sound field radiated from the rear of the pipe (which is negatively scarfed) as can be seen by computing the directivity angle from the inlet to the rear plane which is 120°. As expected from previous work, increased scarf angle reduces the amplitude of the main lobe below the

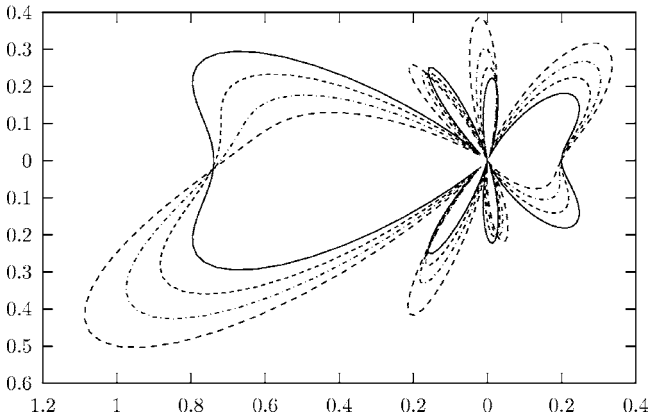

FIG. 6. Polar plot of $|p|^2R^2$ against ϕ at $\theta=\pi/4$ for an axisymmetric field incident on a linear scarf. Wave number $k=1.0$; scarf angles 0°, 15°, 30°, and 45°, shown as solid, dashed, dot-dashed, and dashed lines, respectively.

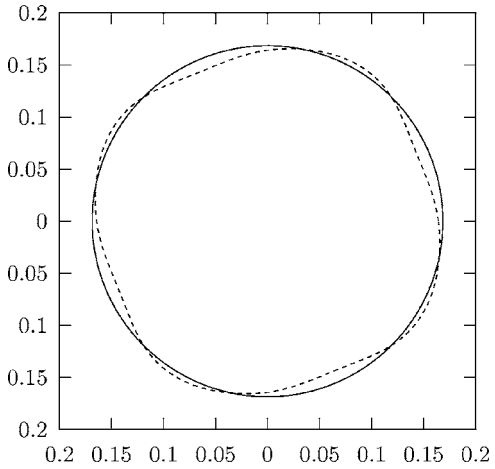

FIG. 7. Polar plot of $|p|^2R^2$ against θ at $\phi=\pi/4$ for field of azimuthal order $m=4$ incident on a four-lobed termination, $k=5$, $\epsilon=0$, 0.25, shown as solid and dashed, respectively.

pipe axis at the expense of an increase above it. Likewise, the narrower lobe in the vertical plane increases above the horizontal but does not reduce significantly below, merely being shifted slightly. The conclusions drawn in earlier work on scarfing are thus confirmed for the large scarf angle considered here.

B. Azimuthal mode-lobed nozzle interaction

The second set of results is a calculation of the sound radiated by a mode of nonzero azimuthal order incident on a sinusoidally profiled duct termination, a simple model of a chevron mixer.[2] In this case, $k=5$, which roughly corresponds to sound generated at a frequency of 550 Hz near a nozzle of diameter 1 m. The nozzle profile is $\sin 4\theta$ and its amplitude is $\epsilon=0.25$. As a baseline condition, the source is an axial dipole distribution of radius 1 with azimuthal variation of order $m=4$, positioned outside the nozzle at $z=1$, i.e., one nozzle radius "downstream." For comparison, the same calculation is also performed for modes $m=3$ and $m=5$. As in Fig. 5, the results are plotted as polar directivities $|p|^2R^2$ at $\phi=\pi/4$, with the axisymmetric case superimposed for comparison.

Figures 7–9 show the baseline case $m=4$ and the comparisons at $m=3$ and $m=5$, respectively. The first point is that the lobing, although it increases the radiated sound slightly, has little effect in the $m=4$ and $m=5$ cases. In the $m=3$ case, however, the increase is quite large and there is practically no reduction in any direction.

The reason for this appears to be that the $m=3$ mode is cut-on in the duct at $k=5$, while the $m=4$ and $m=5$ modes are cut-off. The propagatating mode generates a strong scattering response, including the cut-on $m=-1$ mode, which contributes the asymmetry which is apparent in Fig. 8. By contrast, in the other two cases, although the incident modes excite cut-on modes, they do so via a mode which is cut-off in the duct so that the amplitude of the excited modes is quite weak and no great asymmetry is apparent.

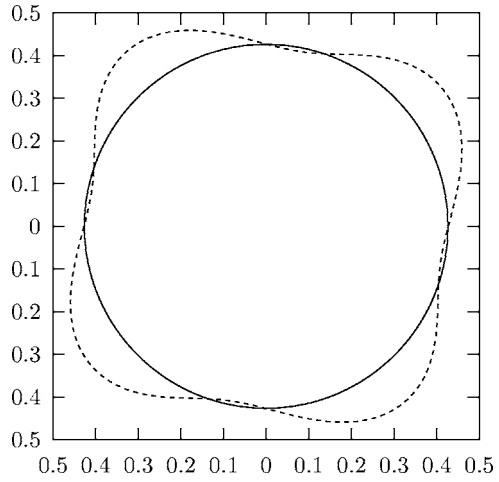

FIG. 8. Polar plot of $|p|^2R^2$ against θ at $\phi=\pi/4$ for field of azimuthal order $m=3$ incident on a four-lobed termination, $k=5$, $\epsilon=0$, 0.25, shown as solid and dashed, respectively.

IV. CONCLUSIONS

A method has been presented for the prediction of scattering by straight circular pipes with arbitrary end profiles. The method has been applied to the problem of radiation of sound from a linearly scarfed duct and to that of scattering by a profile representative of a chevron nozzle on an aeroengine. In the case of the scarfed duct, it was found that there is a limit on the noise reduction benefit to be had by scarfing beyond a certain point. Examination of the sample results for a chevron nozzle has shown that the purely acoustic effect of the end profile depends on the interaction between the internal modes of the pipe and the incident field. The procedure has proven simple to implement using recently developed numerical methods. Future developments might include using a similar approach to model scattering by pipes of almost circular section, or to predict radiation from ducts with asymmetric liners.

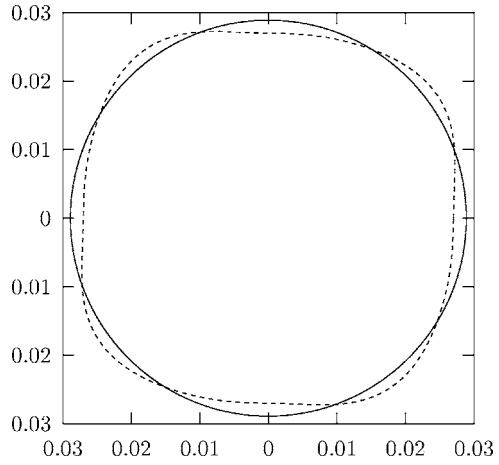

FIG. 9. Polar plot of $|p|^2R^2$ against θ at $\phi=\pi/4$ for field of azimuthal order $m=5$ incident on a four-lobed termination, $k=5$, $\epsilon=0$, 0.25, shown as solid and dashed, respectively.

[1]N. Peake, "On the radiation properties of an asymmetric cylinder," Wave Motion **22**, 371–385 (1995).
[2]J. Bridges and C. A. Brown, "Parametric testing of chevrons on single flow hot jets," in Tenth AIAA/CEAS Aeroacoustics Conference (AIAA, Manchester, UK, 2004), No. AIAA-2004-2824.
[3]R. M. Munt, "The interaction of sound with a subsonic jet issuing from a semi-infinite cylindrical pipe," J. Fluid Mech. **83**(4), 609–640 (1997).
[4]R. Martinez, "Diffracting open-ended pipe treated as a lifting surface," AIAA J. **26**(4), 396–404 (1988).
[5]R. Martinez, "A boundary integral formulation for thin-walled shapes of revolution," J. Acoust. Soc. Am. **87**(2), 523–531 (1990).
[6]M. H. Dunn, J. Tweed, and F. Farassat, "The application of a boundary integral equation method to the prediction of ducted fan engine noise," J. Sound Vib. **227**(5), 1019–1048 (1999).
[7]A. M. Korsunsky, "Gauss-Chebyshev quadrature formulae for strongly singular integrals," Q. Appl. Math. **56**(3), 461–472 (1998).
[8]J. Björkberg and G. Kristensson, "Electromagnetic scattering by a perfectly conducting elliptic disk," Can. J. Phys. **65**, 723–734 (1987).
[9]J. M. Tyler and T. G. Sofrin, "Axial flow compressor noise studies," Trans. Soc. Automotive Eng. **70**, 309–332 (1962).
[10]G. M. Keith and N. Peake, "High-wavenumber acoustic radiation from a thin-walled scarfed cylinder," J. Sound Vib. **255**(1), 147–160 (2002).
[11]D. B. Hanson, "Sound from a propeller at angle of attack: a new theoretical viewpoint," Proc. R. Soc. London, Ser. A **449**, 315–328 (1995).
[12]M. Carley, "The structure of wobbling sound fields," J. Sound Vib. **244**(1), 1–19 (2001).
[13]T. W. Dawson, "On the singularity of the axially symmetric Helmholtz Green's function, with application to BEM," Appl. Math. Model. **19**, 590–599 (1995).
[14]K. W. Mangler, "Improper integrals in theoretical aerodynamics," Current Paper 94, Aeronautical Research Council (unpublished).
[15]M. J. Lighthill, *An Introduction to Fourier Analysis and Generalised Functions* (Cambridge University Press, Cambridge, 1958).
[16]M. P. Brandão, "Improper integrals in theoretical aerodynamics: The problem revisited," AIAA J. **25**(9), 1258–1260 (1987).
[17]G. Monegato, "Numerical evaluation of hypersingular integrals," J. Comput. Appl. Math. **50**, 9–31 (1994).
[18]I. Gradshteyn and I. M. Ryzhik, *Table of Integrals, Series and Products*, 5th ed. (Academic, London, 1980).
[19]M. Frigo and S. G. Johnson, "The design and implementation of FFTW3," Proc. IEEE **93**(2), 216–231 (2005).
[20]A. D. Pierce, *Acoustics: An Introduction to its Physical Principles and Applications* (Acoustical Society of America, New York, 1989).